Paper originally presented at the IAF Global Space Conference on Climate Change (GLOC 2023), 23-25 May 2023, Oslo, Norway. https://www.iafastro.org/

Monitoring of Sea Ice Concentration, Area, and Extent in the polar regions : 40+ years of data from EUMETSAT OSI SAF and ESA CCI

Thomas Lavergne[a]*, Atle Sørensen[a], Rasmus Tonboe[b], Courtenay Strong[c], Matilde Kreiner[d], Roberto Saldo[b], Anton Birkedal[d], Fabrizio Baordo[d], Jozef Rusin[a,e], Trygve Aspenes[a], Steinar Eastwood[a]

[a] *Norwegian Meteorological Institute, Oslo, Norway*
[b] *Technical University of Denmark, Lyngby, Denmark*
[c] *University of Utah, Salt Lake City, Utah, United States of America*
[d] *Danish Meteorological Institute, Copenhagen, Denmark*
[e] *UiT The Arctic University of Norway, Tromsø, Norway*
* Corresponding Author (thomas.lavergne@met.no)

Abstract
The 40+ years long time-series of Arctic and Antarctic sea-ice extent (SIE) and area (SIA) are headline indicators of climate change. The interested public follows their seasonal evolution and record low and high values on online trackers, and climate scientists benchmark their model systems against them. These climate indicators are based on multi-mission data records of sea-ice concentration (SIC), themselves derived from brightness temperature measurements by microwave radiometer satellite missions since the 1970s. Over the past few years, we conducted a coordinated R&D effort from the EUMETSAT Ocean and Sea Ice Satellite Application Facility (OSI SAF) and the ESA Climate Change Initiative (CCI) programme. It has resulted in a collection of state-of-the-art sea-ice concentration climate data records, and their operational extensions. Version 3 of this data was released in 2022/23, and was successfully transferred to the Copernicus Marine (CMEMS) and Climate Change Service (C3S). The previous version (released in 2017) informed the IPCC Assessment Report 6 cycle, and is used in the C3S reanalyses. In this contribution, we introduce the latest version of these SIC CDRs. We present key elements of the algorithm baseline as well as characteristics of the products. The algorithm baseline was designed to ensure climate consistency across the satellite missions, and to avoid potential artificial trends in the input and auxiliary data. The algorithms include 1) reduction of the retrieval uncertainties using Radiative Transfer Models, 2) dynamical tuning of the algorithms and their tie-points, and 3) per-pixel uncertainties. Specific R&D during CCI+ project led to an improved spatial resolution of the SIC data record, exploiting the near-90 GHz imagery channels available since the early 1990s. The product files are designed with several user communities in mind, and allow e.g. accessing "raw" SIC data (before the last filters are applied) for easing Validation and Data Assimilation.

Keywords: Sea Ice Concentration, Climate Data Records, EUMETSAT OSI SAF, ESA CCI, Microwave Radiometry, GLOC 2023, Essential Climate Variable

1. Introduction

Polar sea ice is an integral part of Earth's climate system, and key to marine ecosystems and people living there. Sea Ice Concentration (SIC) is one of the seven parameters in the Sea Ice Essential Climate Variable (ECV) as defined by the Global Climate Observing System (GCOS) [1, 2]. Sea Ice Area (SIA) and Extent (SIE), both derived from SIC, are headline indicators of climate change [3].

Space-borne microwave radiometry has been the workhorse for monitoring SIC over the past 40+ years, allowing daily coverage of polar sea ice at coarse (~50 km) to medium (~10 km) resolution depending on the satellite mission.

In this paper, we present a collection of global (Arctic and Antarctic) SIC Climate Data Records (CDR) and Interim Climate Data Records (ICDR) released by the EUMETSAT Ocean and Sea Ice Satellite Application Facility (OSI SAF) and the ESA Climate Change Initiative (CCI+) in years 2022/23. This is the third release of such SIC CDRs by these projects, building on [4] (around 2010) and [5] (around 2017).

The four CDRs and ICDRs covered here are:

- OSI-450-a : SIC CDR (1978 – 2020) released by OSI SAF, 25 km, based on SMMR, SSM/I, and SSMIS. 10.15770/EUM_SAF_OSI_0013
- OSI-430-a : SIC ICDR (2021 onwards) processed by OSI SAF based on SSMIS. Extends OSI-450-a. 10.15770/EUM_SAF_OSI_0014
- OSI-458 : SIC CDR based on AMSR-E (2002 – 2011) and AMSR2 (2012 – 2020). 25 km. 10.15770/EUM_SAF_OSI_0015
- SICCI-HR-SIC : SIC CDR (1991 – 2020) released by ESA CCI, 12.5 km, based on SSM/I and SSMIS. 10.5285/eade27004395466aaa006135e1b2ad1a

We briefly describe the new input data and R&D that went into this third version (*shortened* v3), compared to the previous version (*shortened* v2). Refer to [5] for a description of the v2 baseline. Detailed information about v3 are also in the associated Algorithm Theoretical Basis Document (ATBD), product user's manual, and validation reports, all accessible from the DOI landing pages.

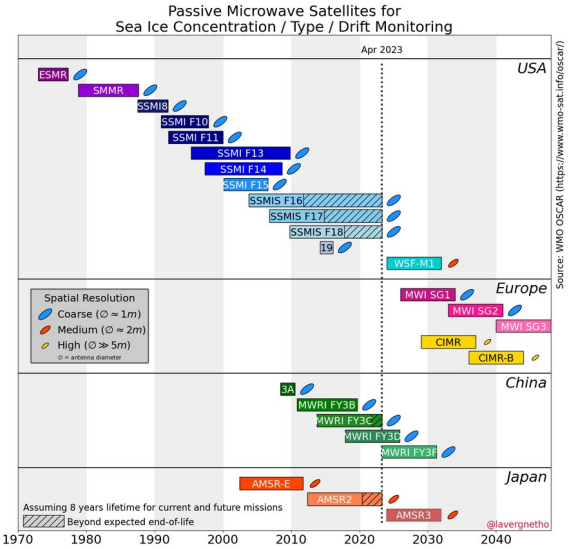

Fig. 1: Timeline of the Passive Microwave satellite missions relevant for sea-ice concentration monitoring with an indication of their spatial resolution capabilities. The CCI+ Sea Ice Phase 1 "v3" CDRs use the SSM/I (from F10) and the SSMIS (F16-F18). The horizontal bars are coloured by sensor family. Credit: T. Lavergne.

2. Input data

OSI-450-a and SICCI-HR-SIC uses R4 of the Fundamental Climate Data Record (FCDR) for SMMR, SSM/I and SSMIS (Fig. 1) released by the Climate Monitoring SAF. OSI-458 uses V002 of the AMSR-E FCDR from NSIDC, and the archive of AMSR2 L1R files from JAXA. The ICDR OSI-430-a uses SSMIS SDR files from NOAA CLASS (Fig. 1).

All v3 CDRs use auxiliary fields from the C3S/ECMWF reanalysis ERA5 (v2 used ERA-Interim). The ICDR uses operational analysis and forecast (IFS) from ECMWF.

3. Algorithms and processing steps

As in v2, we use dynamically-tuned hybrid SIC algorithms. These tune their tie-points and coefficients to minimize the retrieval uncertainty at 0 % SIC and 100% SIC. As in v2, we use the Wentz et al. Radiative Transfer Models (RTM) with fields from a Numerical weather Prediction (NWP) model to correct the brightness temperatures (Tbs) for the contribution of atmosphere to the signal.

Two algorithms are used: SICCI3LF based on Ku (~19 GHz) and Ka (~37 GHz) imagery, and N90LIN based only on the near-90 GHz imagery. SICCI3LF has coarser spatial resolution than N90LIN. But SICCI3LF has lower retrieval uncertainty than N90LIN [6].

New CCI R&D for SICCI-HR-SIC is the use of a pan-sharpening algorithm to improve the resolution of SICCI3LF by using N90LIN as the sharpener. This results in the reSICCI3LF algorithm with (almost) the fine spatial resolution of N90LIN and (almost) the low retrieval uncertainty of SICCI3LF.

Fig. 2 gives an overview of the data flow to prepare OSI-450-a (in the OSI SAF) and SICCI-HR-SIC (in the ESA CCI) and how the two data records are linked. Not shown, the data flow for OSI-458 and OSI-430-a (both in OSI SAF) is similar to that of OSI-450-a.

Fig. 3 shows an example SIC field from OSI-450-a, OSI-458, and SICCI-HR-SIC. Not shown, the ICDR OSI-430-a would be similar to OSI-450-a. The finer spatial resolution of OSI-458 and SICCI-HR-SIC compared to that of OSI-450-a is evident from these panels. OSI-458 uses the more recent AMSR-E and AMSR2 missions to achieve this resolution directly from the SICCI3LF algorithm. SICCI-HR-SIC uses reSICCI3LF (SICCI3LF sharpened by N90LIN) and achieves mostly the same resolution (visually). SICCI-HR-SIC is longer than OSI-458 as it covers 1991-2020 without significant gaps.

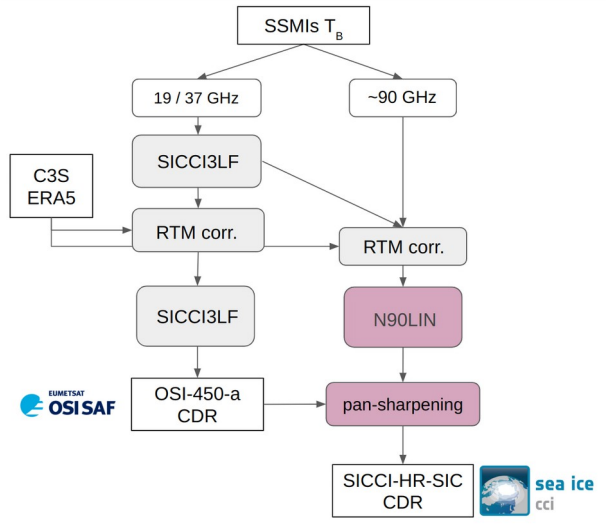

Fig. 2: Schematic of the main algorithmic steps involved in producing OSI-450-a (left) and SICCI-HR-SIC (right), and how the ESA CCI+ process interacts with that of the EUMETSAT OSI SAF.

Many aspects of the processing chains were revisited when preparing the v3 CDRs and we cannot list all the improvements here. A noteworthy R&D input from OSI SAF was to adopt the gap-filling technique of [7] for the Arctic polar observation hole.

4. Scientific validation

All v3 CDRs were validated against the extended SIC Round-Robin Data Package (RRDP) of [8], with a focus on the bias and RMSEs at 0% SIC and 100% SIC. A small positive (+0.5%) bias is observed in the Northern Hemisphere (NH) while the bias is 0% in the Southern Hemisphere (SH). Over consolidated ice (100% SIC) a negative bias of -1% is observed in NH which is not present in the Southern Hemisphere. The bias over 100% SIC conditions is reduced wrt what had been documented with the v2 CDRs [5,9]. The validation also shows a general good agreement between the observed RMSE (validation statistics) and the Mean Total Standard Uncertainty (MTSU) (uncertainties available from the product files). The OSI SAF CDRs were also compared to navigational ice charts from the National Ice Center (NIC).

Algorithms were design to reduce the impact of each of the aspects above, but remaining effects will always be present.

6. File format and data access

All v3 CDRs share the same file format based on the netCDF Climate and Forecast (CF) convention. There are minimal changes wrt the v2 format. Each file contains the main SIC variable `ice_conc`, as well as a number of supporting fields. These include the `total_standard_uncertainty` and its two main contributions (the `algorithm_` and `smearing_` standard uncertainties), a `status_flag` variable, and a SIC variable that holds non-filtered and non-thresholded values (can be below 0% and above 100%) for use in validation and expert users (e.g. data assimilation): `raw_ice_conc_values`.

The v3 CDRs can be accessed through a variety of protocols including FTP, THREDDS, OpenDap, etc… from the OSI SAF webpages and the CCI Open Data Portal. The most direct access to the CDRs and their documentation is using their DOIs (see the list at the end of the Introduction).

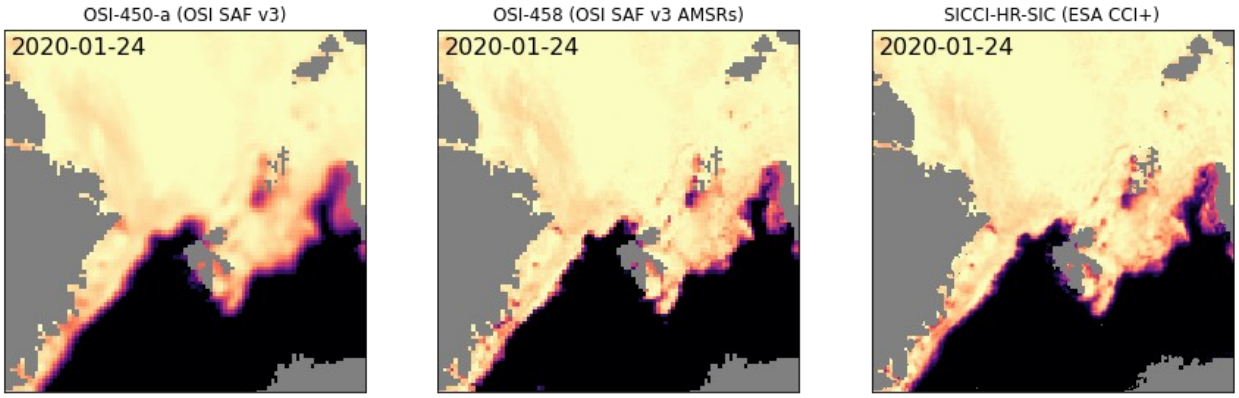

Fig. 3: Example SIC field in the Svalbard and Barents Sea region on 24th January 2020 from OSI-450-a (left), OSI-458 (middle), and SICCI-HR-SIC (right).

5. Caveats and Known Limitations

Being based on passive microwave signal, the v3 CDRs present a number of caveats and limitations that potential users should be aware of when using the products. Most of them are also present in other CDRs based on the same type of satellites, such as those of US NSIDC.

The reader is referred to [5, section 4.3] for an overview of some of the main caveats, that include 1) removal of some true ice along the ice edge by the open water filter, 2) impact of surface melt and melt ponds on the retrieved SICs, 3) underestimation of thin sea ice (< 30 cm), 4) potential for reporting false sea ice along the coasts and in fjords because of the coarse resolution of the sensor.

7. Conclusions

We introduce four SIC CDRs released by the EUMETSAT OSI SAF and the ESA CCI+ programme in 2022/23. These v3 CDRs are OSI-450-a, OSI-458, OSI-430-a, and SICCI-HR-SIC. The CDRs are based on the 40+ long record of space-borne microwave radiometry. The CDRs share many algorithms and processing details. Still, they have various strengths and weaknesses and the potential to address different user needs. Notably, OSI-450-a (extended by OSI-430-a) is a state-of-the-art 40+ years CDRs at coarse resolution (25 km grid spacing), while SICCI-HR-SIC is an advanced enhanced-resolution CDR (12.5 km grid spacing) covering 30 years. The improved resolution of SICCI-HR-SIC is not only visible in daily SIC fields (Fig. 3)

but also in monthly climate anomalies (Fig. 4) which opens interesting prospects for better understanding regional patterns of the climate system.

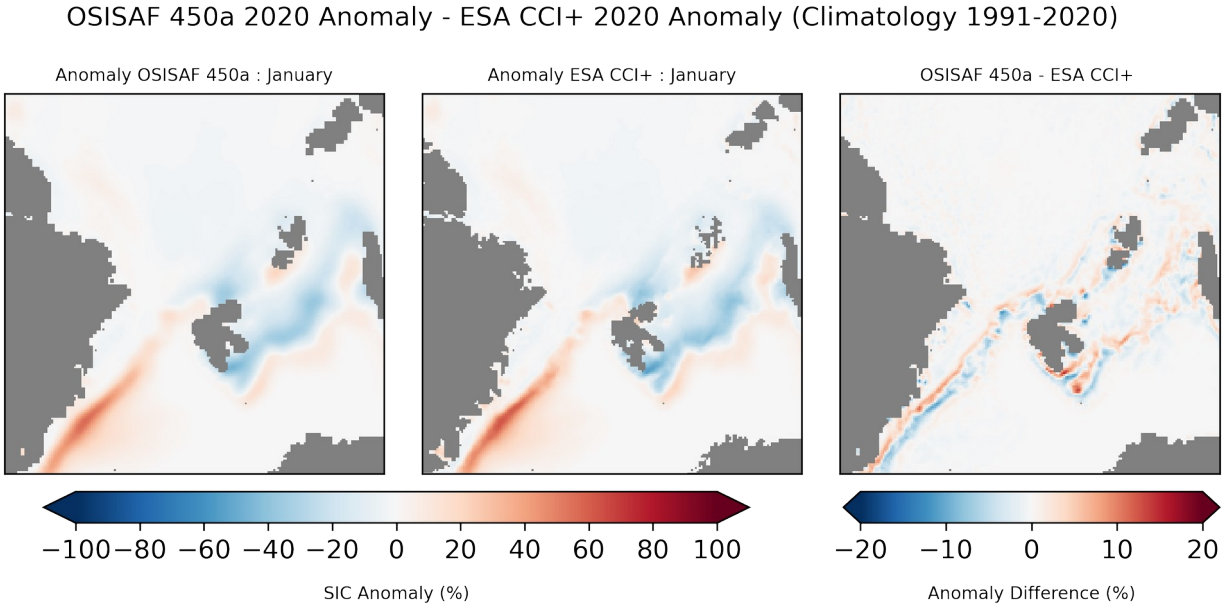

Fig. 4: Monthly anomaly for January 2020 for OSI-450-a (left), SICCI-HR-SIC (middle) and the difference of the two anomaly maps (right). The anomalies are wrt the wrt their respective 1991-2020 climatology.

Acknowledgements

The R&D, production, and validation of these SIC CDRs was supported by the EUMETSAT OSI SAF (Continuous Developments and Operations Phase 3), and the ESA Climate Change Initiative (CCI+) Phase 1 Sea Ice project (ESA contract 4000126449/19/I-NB).

We are grateful for the providers of the data we used as input for these CDRs, including CM SAF, US NSIDC, JAXA, and C3S/ECMWF.

References

[1] Lavergne, Thomas, Stefan Kern, Signe Aaboe, Lauren Derby, Gorm Dybkjaer, Gilles Garric, Petra Heil, Stefan Hendricks, Jürgen Holfort, Stephen Howell, Jeffrey Key, Jan L Lieser, Ted Maksym, Wieslaw Maslowski, Walt Meier, Joaquín Muñoz-Sabater, Julien Nicolas, Burcu Özsoy, Benjamin Rabe, Wolfgang Rack, Marilyn Raphael, Patricia de Rosnay, Vasily Smolyanitsky, Steffen Tietsche, Jinro Ukita, Marcello Vichi, Penelope Wagner, Sascha Willmes, and Xi Zhao. "A New Structure for the Sea Ice Essential Climate Variables of the Global Climate Observing System". Bulletin of the American Meteorological Society 103.6 (2022): E1502-E1521. https://doi.org/10.1175/BAMS-D-21-0227.1 Web.

[2] Global Climate Observing System: The 2022 GCOS Implementation Plan, GCOS No. 244, World Meteorological Organization (WMO), Geneva, Switzerland, 2022a.

[3] Trewin, Blair, Anny Cazenave, Stephen Howell, Matthias Huss, Kirsten Isensee, Matthew D. Palmer, Oksana Tarasova, and Alex Vermeulen. "Headline Indicators for Global Climate Monitoring". Bulletin of the American Meteorological Society 102.1 (2021): E20-E37. https://doi.org/10.1175/BAMS-D-19-0196.1 Web.

[4] Tonboe, R. T., Eastwood, S., Lavergne, T., Sørensen, A. M., Rathmann, N., Dybkjær, G., Pedersen, L. T., Høyer, J. L., and Kern, S.: The EUMETSAT sea ice concentration climate data record, The Cryosphere, 10, 2275–2290, https://doi.org/10.5194/tc-10-2275-2016, 2016.

[5] Lavergne, T., Sørensen, A. M., Kern, S., Tonboe, R., Notz, D., Aaboe, S., Bell, L., Dybkjær, G., Eastwood, S., Gabarro, C., Heygster, G., Killie, M. A., Brandt Kreiner, M., Lavelle, J., Saldo, R., Sandven, S., and Pedersen, L. T.: Version 2 of the EUMETSAT OSI SAF and ESA CCI sea-ice concentration climate data records, The Cryosphere, 13, 49–78, https://doi.org/10.5194/tc-13-49-2019, 2019.

[6] Ivanova, N., Pedersen, L. T., Tonboe, R. T., Kern, S., Heygster, G., Lavergne, T., Sørensen, A., Saldo, R., Dybkjær, G., Brucker, L., and Shokr, M.: Inter-

comparison and evaluation of sea ice algorithms: towards further identification of challenges and optimal approach using passive microwave observations, The Cryosphere, 9, 1797–1817, https://doi.org/10.5194/tc-9-1797-2015, 2015.

[7] Strong C, Golden KM. Filling the Polar Data Gap in Sea Ice Concentration Fields Using Partial Differential Equations. Remote Sensing. 2016; 8(6):442. https://doi.org/10.3390/rs8060442

[8] Pedersen, Leif Toudal; Saldo, Roberto; Ivanova, Natalia; Kern, Stefan; Heygster, Georg; Tonboe, Rasmus; et al. (2019): Reference dataset for sea ice concentration. figshare. Dataset. https://doi.org/10.6084/m9.figshare.6626549.v7

[9] Kern, S., Lavergne, T., Notz, D., Pedersen, L. T., Tonboe, R. T., Saldo, R., and Sørensen, A. M.: Satellite passive microwave sea-ice concentration data set intercomparison: closed ice and ship-based observations, The Cryosphere, 13, 3261–3307, https://doi.org/10.5194/tc-13-3261-2019, 2019.